



## Short Communication

Corrosion behavior of the  $\zeta$ -CrZn<sub>13</sub> phase obtained by annealing an electrodeposited Zn-Cr coatingV. Chakarova<sup>a</sup>, Tz. Boiadjeva-Scherzer<sup>b</sup>, D. Kovacheva<sup>c</sup>, H. Kronberger<sup>d</sup>, M. Monev<sup>a,\*</sup><sup>a</sup> Institute of Physical Chemistry, Bulgarian Academy of Sciences, Acad G. Bonchev Str., Bl.11, Sofia 1113, Bulgaria<sup>b</sup> Centre of Electrochemical Surface Technology GmbH, Viktor-Kaplan-Straße 2, 2700 Wiener Neustadt, Austria<sup>c</sup> Institute of General and Inorganic Chemistry, Bulgarian Academy of Sciences, Acad G. Bonchev Str., Bl.11, Sofia 1113, Bulgaria<sup>d</sup> TU-Wienna, Institute for Chemical Technology and Analytics, Getreidemarkt 9/164ec, A-1060 Vienna, Austria

## ARTICLE INFO

## Keywords:

Electrodeposited Zn-Cr alloy

 $\zeta$ -CrZn<sub>13</sub> phase

Corrosion

Anodic dissolution

## ABSTRACT

Electrodeposited and physically vapor-deposited Zn-Cr alloy coatings consist of several non-equilibrium Zn-Cr phases – hexagonal  $\eta$ -(Zn, Cr), hexagonal  $\delta$ -(Zn, Cr), and cubic  $\Gamma$ -(Zn, Cr) – which have different corrosion characteristics. Upon annealing, these non-equilibrium phases transform into  $\zeta$ -CrZn<sub>13</sub> phase and  $\eta$ -Zn or  $\alpha$ -Cr, depending on the Cr content of the alloys. A layer solely composed of the  $\zeta$ -CrZn<sub>13</sub> phase can be obtained from a certain stoichiometric composition of the starting alloy. In the present work the corrosion behavior of a layer composed solely of the  $\zeta$ -CrZn<sub>13</sub> phase is studied for the first time. This phase is obtained by annealing a Zn-5.6% Cr alloy coating ( $\eta$ -(Zn, Cr) phase) electrodeposited on steel. Electrochemical and corrosion studies revealed a more positive corrosion potential in 0.5 M Na<sub>2</sub>SO<sub>4</sub> solution (at pH 5.9) and less weight loss (at pH 1.3) of the thermally treated coating as well as more regular corrosion compared to the as-deposited layer. The changes in the morphology and phase composition of the alloy layer occurring as a result of annealing, and the effect on corrosion, are studied using SEM and XRD.

## 1. Introduction

Zn-Cr alloy coatings are of interest mainly due to their corrosion-protection properties, which some authors associate directly with the phase composition of the alloy [1]. A brief review of the literature on the ability of alloys with different Cr content and different phase compositions to protect against corrosion is given in [2].

The subject of the present study is the corrosion/electrochemical behavior of the phase  $\zeta$ -CrZn<sub>13</sub>. The existence of  $\zeta$ -CrZn<sub>13</sub> in electrodeposited Zn-Cr alloys can be detected after thermal treatment [3]. Upon annealing electrodeposited Zn-Cr coatings at 260 °C for 90 min, coatings with 0.8 mass % Cr transform into a hexagonal (hcp)  $\eta$ -Zn phase, while those with >5.7 mass % Cr transform to the  $\zeta$ -(Zn,Cr) phase, which has a CoZn<sub>13</sub>-type structure. Such a transition has also been shown for vacuum-evaporated coatings [4]. Heating the hcp  $\delta$ -(Zn, Cr) phase above 170 °C results in an irreversible phase change to monoclinic  $\zeta$ -CrZn<sub>13</sub>. The time required for complete transformation at 230 °C is 20 min.

The phase transition effect is used to obtain a two-layer coating with good adhesion to the steel substrate [5]. The authors also indicate

increased corrosion protection of a coating containing predominantly the  $\zeta$ -CrZn<sub>13</sub> phase compared to a coating of the same thickness and composition, but mainly comprising the  $\delta$ -(Zn, Cr) phase. However, no corrosion/electrochemical studies of coatings consisting of the  $\zeta$ -CrZn<sub>13</sub> phase have yet been performed.

Our previous work was devoted to investigation of the corrosion behavior of as-deposited Zn-Cr alloy coatings with different Cr content in sulphate media of different acidity [6]. In a later paper, the influence of the annealing temperature on the transition to the  $\zeta$ -CrZn<sub>13</sub> phase in electrodeposited Zn-Cr alloy coatings containing 3.6; 5.4 or 9.4 mass % Cr was investigated using DSC and XRD [7]. In all three alloys, an irreversible transition was observed. On increasing the Cr content, the beginning of the transition is shifted to a higher temperature – from 180 to 250 °C. After annealing, the sample with an average Cr content of 5.4 mass % contains traces of a residual  $\eta$ -Zn phase. Therefore, a Zn-Cr alloy coating with an average Cr content of 5.6 mass % was selected for the present investigations. This composition is close to the stoichiometric composition of the phase  $\zeta$ -CrZn<sub>13</sub>.

\* Corresponding author.

E-mail address: [monev@ipc.bas.bg](mailto:monev@ipc.bas.bg) (M. Monev).<https://doi.org/10.1016/j.elecom.2020.106904>

Received 2 October 2020; Received in revised form 8 December 2020; Accepted 15 December 2020

Available online 21 December 2020

1388-2481/© 2020 The Authors.

Published by Elsevier B.V. This is an open access article under the CC BY-NC-ND license

<http://creativecommons.org/licenses/by-nc-nd/4.0/>.

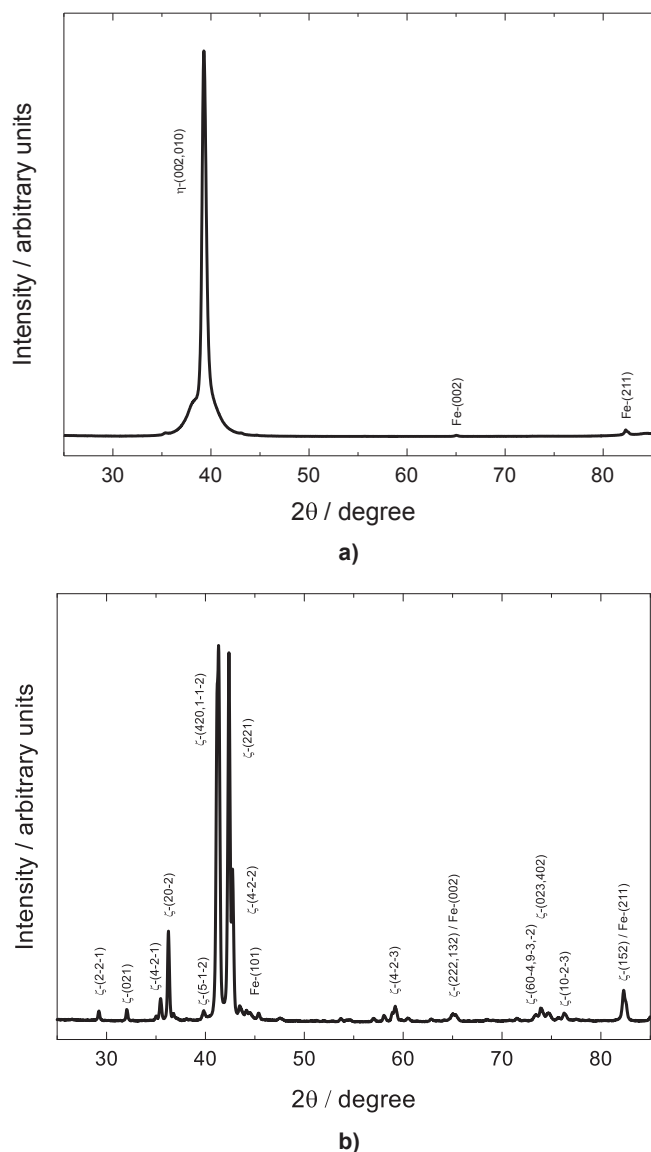


Fig. 1. XRD patterns of a Zn-5.6%Cr alloy coating obtained (a) before and (b) after annealing in a laboratory dryer at 210 °C for 1 h.

## 2. Experimental

Zn-5.6%Cr alloy coatings were electrodeposited from an electrolyte containing 40 g l<sup>-1</sup> Zn, 15 g l<sup>-1</sup> Cr (added as sulphates) and 1 g l<sup>-1</sup> PEG 6000, pH 1.8, in a flow cell (flow rate 2.7 m s<sup>-1</sup>, current density 85 A dm<sup>-2</sup>, electrolyte temperature 56 °C) onto mild steel substrates with a thickness of 70 μm. The Zn-Cr coatings had an average thickness of 5.1 μm.

The corrosion tests were carried out in 0.5 M Na<sub>2</sub>SO<sub>4</sub> solution at a temperature of 25 °C. The pH of this solution was adjusted to pH 1.3 by addition of H<sub>2</sub>SO<sub>4</sub>. Samples with a working surface area of 0.785 cm<sup>2</sup> were immersed in the solution for 3 min and thereafter their weight loss

Table 1

Effect of the annealing on the corrosion of Zn-5.6%Cr alloy coating. Dissolution for 3 min in 0.5 M Na<sub>2</sub>SO<sub>4</sub>, pH 1.3.

Dissolved amount of:	AAA/mg l <sup>-1</sup>	
	Zn	Cr
Zn-5.6%Cr (as-deposited)	54.1	1.65 (3.0%)
Zn-5.6%Cr (annealed)	24.5	1.50 (5.8%)

was determined. After the corrosion tests, samples of the Na<sub>2</sub>SO<sub>4</sub> solution were examined by atomic-absorption analysis (AAA) and the dissolved amounts of Zn and Cr were analyzed.

Open circuit potential (OCP) transients were plotted in 0.5 M Na<sub>2</sub>SO<sub>4</sub> solution of pH 5.9. Potentiodynamic polarization with a scan rate of 1 mV s<sup>-1</sup> was applied in order to study the anodic dissolution of the coatings. The investigations were performed in a three-electrode cell with a volume of 50 ml. The cell was equipped with a reference Hg/Hg<sub>2</sub>SO<sub>4</sub> electrode, a working electrode with a surface area of 0.2 cm<sup>2</sup> and a Pt counter electrode. The reference electrode was connected to the cell through a Haber-Luggin capillary tip. All electrochemical experiments were carried out using a potentiostat/galvanostat model 263A (EG&G Princeton Applied Research). The corrosion potential ( $E_{\text{corr}}$ ) and polarization resistance ( $R_p$ ) were calculated from the data collected during the potentiodynamic polarization measurements using SoftCorr II software.

The changes in the thickness of the coatings and in the Cr content of the alloys before and after corrosion treatment were followed by means of X-ray fluorescence analysis (XRFA) (Fischerscope XDL-B, Software WinFTM 6.09) and energy-dispersive X-ray microanalysis (EDX).

The surface morphology of the coatings was studied by scanning electron microscopy (SEM) (JEOL JSM 733).

X-ray powder diffraction patterns were collected within the range 2θ = 10–100° with a constant step of 0.02° using a Bruker D8 Advance diffractometer with CuK<sub>α</sub> radiation and a LynxEye detector. Unit cell parameters were determined with the Topas-4.2 software package using the fundamental parameters peak-shape description including appropriate corrections for instrumental broadening and diffractometer geometry.

## 3. Results and discussion

### 3.1. XRD analysis of Zn-5.6%Cr alloy coating annealed in a laboratory dryer

The investigations described in a previous work showed that in the case of the alloy coating Zn-5.4%Cr, the transition to ζ-CrZn<sub>13</sub> phase is completed at a temperature of 180 °C [7]. Such a temperature can be realized in a laboratory dryer, which is an environment similar to the real conditions of technological processing of galvanized steel sheet in a non-protective atmosphere.

Fig. 1 presents a comparison between the diffraction patterns of the Zn-5.6%Cr sample before and after annealing in a laboratory dryer at 210 °C for 1 h. The XRD pattern of the as-deposited coating exhibits peaks attributed to the η-(Zn, Cr) phase ( $a = 2.637(2)$  Å;  $c = 4.742(3)$  Å) with a preferred orientation of (010) direction perpendicular to the sample plane. During annealing, the η-(Zn, Cr) phase is completely transformed into a monoclinic ζ-CrZn<sub>13</sub> phase ( $a = 13.4746(4)$  Å,  $b = 7.6731(4)$  Å,  $c = 5.1610(1)$  Å;  $\beta = 127.877^\circ$  (2)). The size of the crystallites increases from 15 to 20 nm to 90 nm as a result of the thermal treatment.

The XRD data do not indicate the presence of an oxide phase. Reflexes in the angular range 2θ = 70–80° could be related to the interaction of the alloy with the steel substrate. In accordance with the literature data [8], our previous studies [7] have shown that upon annealing to 400 °C, Zn coatings interact with the steel substrate, but with increasing Cr content in the alloy, the interaction weakens and in Zn-9.4%Cr alloy coatings it is no longer observed. In the present studies, no reflex of the Γ-(Zn, Fe) phase is registered in the indicated range of the diffraction pattern of the annealed sample, and that of the δ-(Zn, Fe) phase coincides with a reflex of the ζ-CrZn<sub>13</sub> phase.

### 3.2. Corrosion investigations of the ζ-CrZn<sub>13</sub> phase

Samples for conducting corrosion tests were cut from a specimen composed of the ζ-CrZn<sub>13</sub> phase, annealed in the laboratory dryer.

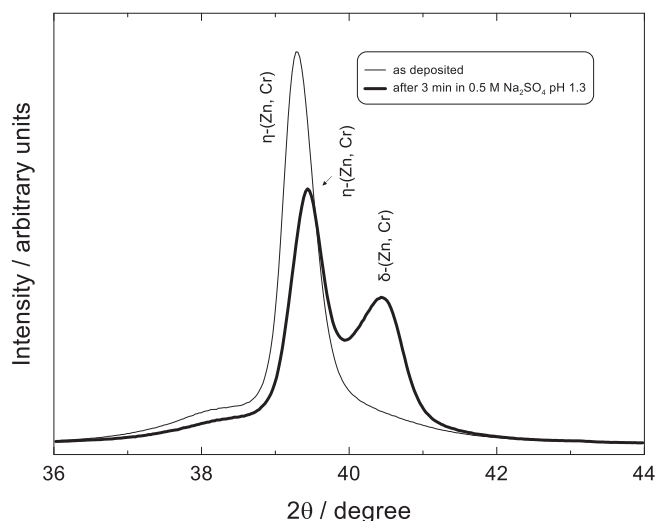


Fig. 2. XRD pattern of an as-deposited Zn-5.6%Cr alloy coating before and after corrosion in 0.5 M Na<sub>2</sub>SO<sub>4</sub>, pH 1.3 for 3 min.

### 3.2.1. Dissolution in 0.5 M Na<sub>2</sub>SO<sub>4</sub>, pH 1.3

The annealed sample dissolves in 0.5 M Na<sub>2</sub>SO<sub>4</sub>, pH 1.3 for 3 min to a lesser extent than the as-deposited sample, as shown in Table 1.

In the column “Cr”, the dissolved amount of Cr related to the total dissolved mass is given in brackets. The data reveal that in the case of the un-annealed sample, Zn is predominantly dissolved, while for the annealed sample the dissolved amount of Cr is proportional to the Cr content in the sample before treatment, suggesting homogeneous corrosion.

After the corrosion treatment of the un-annealed sample, a splitting of the XRD-peak was observed which could be explained by the appearance of two hexagonal phases – η-(Zn, Cr) ( $a = 2.630(1) \text{ \AA}$ ;  $c =$

$4.753(2) \text{ \AA}$ ) and δ-(Zn, Cr) ( $a = 2.702(1) \text{ \AA}$ ;  $c = 4.452(2) \text{ \AA}$ ) (see Fig. 2). The detection of a Cr-enriched phase (δ-(Zn, Cr)) could be related to the preferential dissolution of Zn (Table 1). The parameters of the monoclinic ζ-phase hardly change after the corrosion treatment:  $a = 13.5260(1) \text{ \AA}$ ;  $b = 7.6776(4) \text{ \AA}$ ;  $c = 5.1724(2) \text{ \AA}$  and  $\beta = 127.885^\circ(2)$ .

Fig. 3 shows the morphology of the samples before annealing (a,b), after annealing (d,e) and after corrosion treatment (c,f). After deposition, the coatings are not compact. There is a discontinuity (Fig. 3a), which disappears after annealing and a well-pronounced network of cracks is formed (Fig. 3d). The globular formations occasionally observed on top of the as-deposited sample at higher magnification (Fig. 3b) are dendrites with a chemical composition close to that of the base coating (a slightly lower Cr content of about 5.2 mass %). After annealing, the number of these formations visibly increases (Fig. 3e). EDX analysis of isolated formations showed the presence of 2 to 4 mass % O in addition to Zn and Cr. These values should not be taken unconditionally, as the data include information from a larger volume. However, the detected oxygen content is an indication of the oxidation of the globular formations caused by annealing performed in a non-protective atmosphere.

As seen, after the corrosion treatment in a solution of 0.5 M Na<sub>2</sub>SO<sub>4</sub> (pH 1.3) the corrosion of the un-annealed sample proceeds along the discontinuities (Fig. 3c), while in the annealed sample the surface is corroded (Fig. 3f). The pits on the surface of the annealed sample could be the result of the predominant dissolution of the oxidized dendritic formations, which are active sites, not only of oxidation, but also of corrosion. No crack corrosion/crack expansion is observed.

### 3.2.2. Open circuit potential measurements

Despite there being the same Cr content in the as-deposited and annealed alloy coatings, the reorganization of the crystalline structure, the change in the size of crystallites and the redistribution of Cr are reflected in a difference in the OCP (Fig. 4). The OCP of the annealed alloy coating is about 100 mV more positive than that of the as-

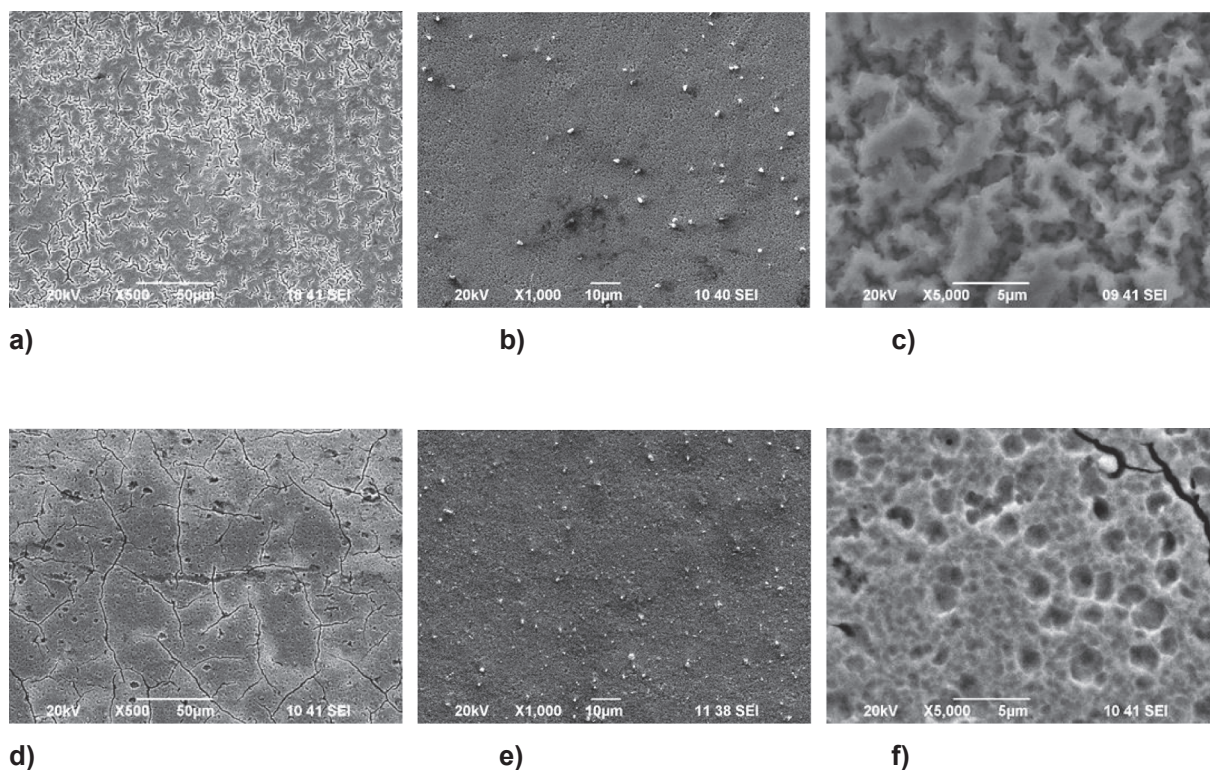


Fig. 3. Morphology of the Zn-5.6%Cr alloy coating (a,d) before and (b,e) after annealing and (c,f) after 3 min in 0.5 M Na<sub>2</sub>SO<sub>4</sub>, pH 1.3. (a,b,c) show the as-deposited coating, (d,e,f) the annealed coating.

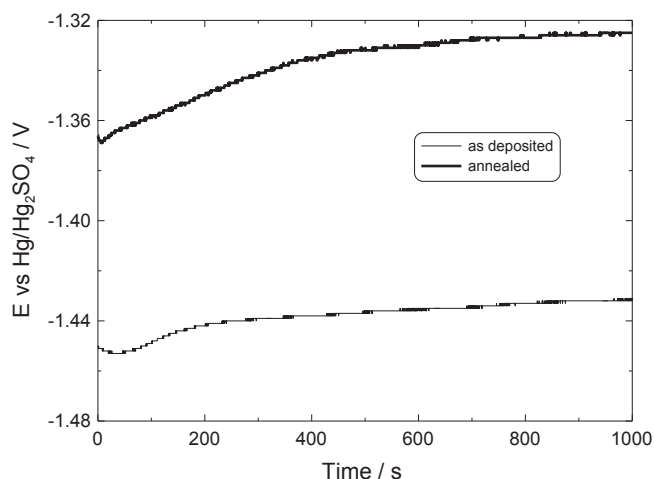


Fig. 4. OCP vs time for as-deposited and annealed Zn-5.6%Cr alloy coatings in 0.5 M Na<sub>2</sub>SO<sub>4</sub> solution, pH 5.9.

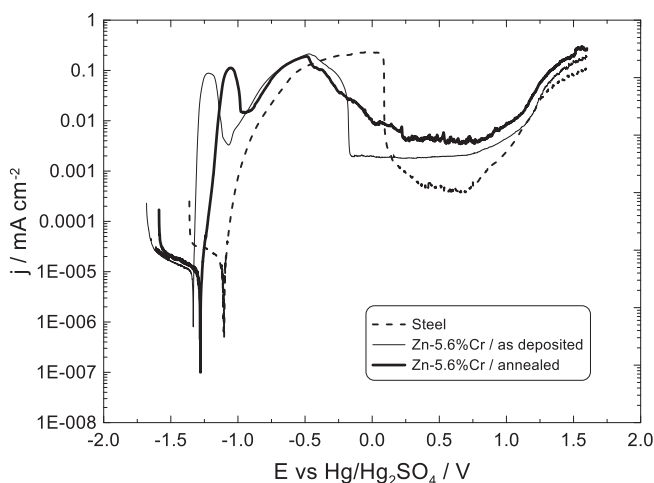


Fig. 5. Potentiodynamic polarization curves of steel, as-deposited and annealed Zn-5.6%Cr alloy coatings in 0.5 M Na<sub>2</sub>SO<sub>4</sub>, pH 5.9.

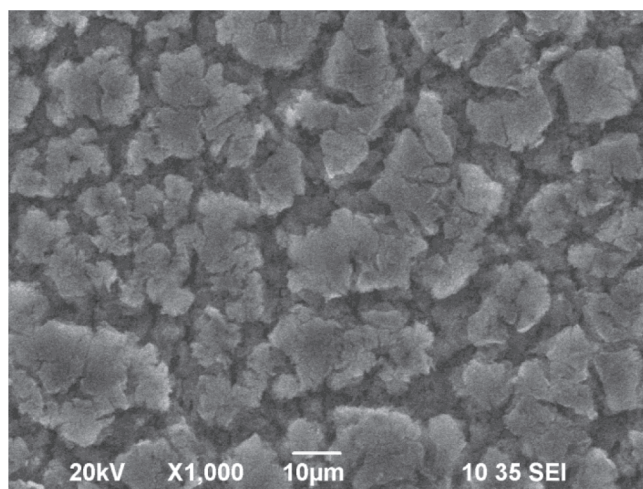
deposited alloy coating.

### 3.2.3. Anodic potentiodynamic polarization curves

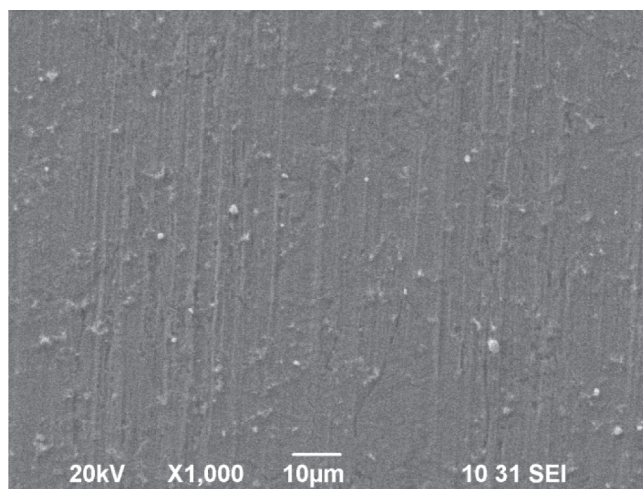
The influence of annealing on the anodic behavior of the Zn-5.6% Cr alloy coating is shown in Fig. 5. To clarify the nature of the anodic maxima, the potentiodynamic curves were interrupted after both the first and second maxima. The treated surface was analyzed by XRFA and the solutions were analyzed by atomic absorption analysis.

In the case of the as-deposited alloy, the first anodic maximum is associated with Zn dissolution. Due to Zn dissolution, a Cr-rich thin layer (up to about 40 mass % Cr) remains on the surface with a corroded structure along the grain boundaries (Fig. 6a). The second anodic maximum is determined mainly by dissolution of the steel substrate. Without a basis, residues from the alloy coating fall into the solution and soon after the second maximum the steel surface remains practically clean. The main feature of this part of the curve is the passivation of the substrate at considerably more negative potentials than for bare, ungalvanized steel, as observed in previous corrosion studies of as-deposited coatings [6].

In general, the polarization curve of the annealed sample is shifted to more positive values of the potential, near to the second anode maximum. The first anode maximum of the annealed alloy is again associated with Zn dissolution, but at a slower rate. The alloy layer



a)



b)

Fig. 6. SEM images of (a) as-deposited and (b) annealed Zn-5.6%Cr samples after potentiodynamic polarization to a potential after the first anodic maximum.

Table 2

Effect of the annealing of the Zn-5.6%Cr alloy coating on the corrosion potential and polarization resistance, measured in 0.5 M Na<sub>2</sub>SO<sub>4</sub>, pH 5.9.

	$E_{\text{corr}}/V$	$R_p/k\Omega \text{ cm}^{-2}$
Zn	-1.49	0.4
Zn-5.6%Cr (as deposited)	-1.38	4.4
Zn-5.6%Cr (annealed)	-1.29	7.3

remaining after the maximum also contains up to about 40 mass % Cr. The morphology of the layer indicates uniform dissolution (Fig. 6b). The ascending part of the second maximum overlaps with the corresponding part of the maximum of the un-annealed sample. Then, a gradual decrease in the corrosion current density is observed, nearly until the onset of the oxygen evolution reaction. After finishing the polarization curve, XRFA registers residuals of the coating on the surface. Average data from the potentiodynamic polarization curves are presented in Table 2.

X-ray analysis after the first anodic maximum shows that even in this mode of dissolution two hexagonal phases appear in the un-annealed sample:  $\eta$  ( $a = 2.6395(4) \text{ \AA}$ ;  $c = 4.732(5) \text{ \AA}$ ) and  $\delta$  ( $a = 2.770(1) \text{ \AA}$ ;  $c$

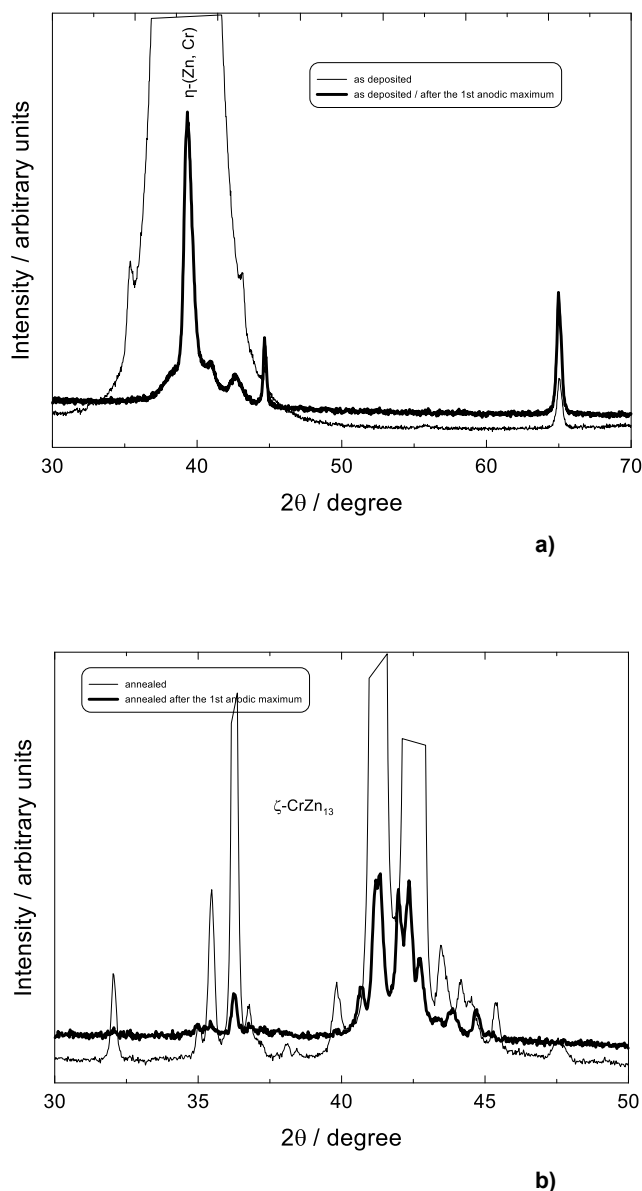


**Fig. 7.** XRD pattern of (a) as-deposited and (b) annealed Zn-5.6%Cr alloy coating before and after the first anodic maximum at anodic potentiodynamic polarization in 0.5 M Na<sub>2</sub>SO<sub>4</sub>, pH 5.9.

= 4.405(2) Å (Fig. 7a).

For the annealed sample, the monoclinic ζ-phase ( $a = 13.50(2)$  Å;  $b = 7.66(1)$  Å;  $c = 5.158(4)$  Å;  $\beta = 127.90^\circ$  (5)) becomes thinner, which is also demonstrated by the increase in the intensity of the reflexes from the substrate (Fig. 7b).

#### 4. Conclusions

After annealing the electrodeposited Zn-5.6% Cr alloy coating in a

laboratory dryer at 210 °C for 1 h, the original hexagonal η-(Zn, Cr) phase of the coating is completely transformed into a monoclinic ζ-CrZn<sub>13</sub> phase.

Subsequent investigations reveal the improved corrosion/electrochemical characteristics ( $E_{\text{corr}}$ ,  $R_p$ , anodic dissolution rate) of the ζ-CrZn<sub>13</sub> coating, compared to those of the as-deposited coating.

Corrosion (in 0.5 M Na<sub>2</sub>SO<sub>4</sub>, pH 1.3) and anodic dissolution (in 0.5 M Na<sub>2</sub>SO<sub>4</sub>, pH 5.9) result in similar changes in the phase composition for as-deposited and annealed coatings. That means a differentiation into two hexagonal Zn-Cr phases in the treated as-deposited coatings as a result of the preferential dissolving of Zn, and a thinner layer of the ζ-CrZn<sub>13</sub> phase with lattice parameters practically identical to those of the starting samples of the annealed coatings.

#### CRediT authorship contribution statement

**V. Chakarova:** Investigation. **Tz. Boiadjieva-Scherzer:** Visualization, Funding acquisition, Investigation, Editing - original draft. **D. Kovacheva:** Investigation. **H. Kronberger:** Funding acquisition. **M. Monev:** Investigation, Conceptualization, Data curation, Writing - original draft, Funding acquisition.

#### Declaration of Competing Interest

The authors declare that they have no known competing financial interests or personal relationships that could have appeared to influence the work reported in this paper.

#### Acknowledgement

These investigations were performed with the support of the Austrian Science Foundation FFG and the governments of Lower Austria and Upper Austria in the frame of the COMET program. The authors would like to thank voestalpine Stahl GmbH, Linz, Austria for providing samples used in the present investigations.

#### References

- [1] H. Nakamaru, T. Fujimura, H. Ohnuma, K. Mochiziku, N. Morito, M. Katayama, US Patent 5 510 196, 1996.
- [2] Tz. Boiadjieva, M. Monev, Chromium alloys: chemistry, production and application, in: B. Franco (Ed.), Electrodeposition, Composition And Properties of Zn-Cr Alloy Coatings, Nova Publishers, New York, 2014, pp. 1–41.
- [3] S. Hashimoto, S. Ando, T. Urakawa, M. Sagiya, J. Japan. Inst. Metals 62 (1998) 9–14, [https://doi.org/10.2320/jinstmet1952.62.1\\_9](https://doi.org/10.2320/jinstmet1952.62.1_9).
- [4] C. Scott, C. Olier, A. Lamande, P. Choquet, D. Chaleix, Thin Solid Films 436 (2003) 232–237, [https://doi.org/10.1016/S0040-6090\(03\)00597-2](https://doi.org/10.1016/S0040-6090(03)00597-2).
- [5] D. Chaleix, P. Choquet, A. Lamande, C. Scott, C. Olier, US Patent 6 682 828 B2, 2004.
- [6] V. Chakarova, Tz. Boiadjieva-Scherzer, D. Kovacheva, H. Kronberger, M. Monev, Corr. Sci. 140 (2018) 73–78, <https://doi.org/10.1016/j.corsci.2018.06.019>.
- [7] Tz. Boiadjieva-Scherzer, G. Avdeev, Ts. Vassilev, V. Chakarova, H. Kronberger, M. Monev, Surf. Eng. 35 (2019) 1055–1060, <https://doi.org/10.1080/02670844.2019.1598023>.
- [8] S. Wienströer, M. Fransen, H. Mittelstädt, C. Nazikkol, M. Völker, International centre for diffraction data, Adv. X-ray Anal. 46 (2003) 291–296.